

# Abelian dark matter models for 511 keV $\gamma$ rays and direct detection

James M. Cline<sup>1</sup> \* and Andrew R. Frey<sup>2</sup> \*\*

<sup>1</sup> Department of Physics, McGill University, Montréal, QC, H3A 2T8, Canada

<sup>2</sup> Dept. of Physics and Winnipeg Institute for Theoretical Physics, University of Winnipeg, Winnipeg, MB, R3B 2E9, Canada

**Key words** dark matter, galactic gamma rays, heavy photons, hidden sector models

We construct a simple U(1) hidden sector model of metastable dark matter that could explain excess 511 keV gamma rays from the galactic center as observed by INTEGRAL, through inelastic scattering of dark matter followed by its decay. Although the model is highly constrained, it naturally accommodates dark matter with mass and cross section in the range suggested by the CoGeNT and CRESST experiments. The dark gauge boson that mediates the interactions with standard model matter has a mass of several hundred MeV, and might be discovered by heavy photon detection experiments, including APEX, MAMI and HPS.

## Contents

<b>1</b>	<b>Introduction</b>	<b>1</b>
<b>2</b>	<b>Defining the model</b>	<b>3</b>
<b>3</b>	<b>The 511 keV signal and relic density</b>	<b>4</b>
3.1	Scattering rate for $e^+$ production . . . . .	5
3.2	Relic density . . . . .	6
3.3	Relations between model parameters . . . . .	9
<b>4</b>	<b>Other constraints</b>	<b>9</b>
4.1	Lifetimes of excited states . . . . .	9
4.2	Washout of metastable states . . . . .	10
	Kinetic before chemical freezeout? . . . . .	12
4.3	Astrophysical Constraints . . . . .	12
<b>5</b>	<b>Direct detection</b>	<b>13</b>
<b>6</b>	<b>Conclusions</b>	<b>14</b>
	<b>References</b>	<b>15</b>

## 1 Introduction

While direct detection of dark matter (DM) is presently an urgent endeavor, it is possible that indirect signals of DM have already been seen. Most recently the detections of excess high-energy galactic electrons and positrons by the PAMELA [1] and Fermi/LAT [2] experiments have stimulated such interest (although this signal is now generally believed to be due to pulsars), but there is a much longer-standing observation originally from [3, 4] of excess 511 keV gamma rays

\* email: jcline@physics.mcgill.ca

\*\* Corresponding author email: a.frey@uwinnipeg.ca, phone: +1-204-786-9215, fax: +1-204-774-4134

from the galactic center (studied in the greatest detail by INTEGRAL/SPI [5–8]), which might be explained by positrons from DM decays. This possibility is especially interesting because there is no widely accepted astrophysical explanation for the observation [9–19].

Proposed astrophysical explanations for the excess 511 keV gamma rays include pulsars, X-ray binaries, violent events near the galactic black hole (Sgr A\*), and radionuclides from supernovae and massive stars; [20] gives a thorough review and critical appraisal of these proposals, including DM proposals, as well as a discussion of the effects of positron propagation. An important morphological feature of the 511 keV emission, which is difficult to reproduce with steady-state astrophysical models, is that the galactic bulge is several times brighter than the disk. As an example, consider positron production by radionuclides, which has been claimed as an explanation of the entire 511 keV signal by [17, 18] based on a particular model of radionuclide production and positron production with very specific assumptions. However, [21] recently argued that, for updated models of radionuclide production, reasonable assumptions about positron production cannot reproduce the observed bulge-to-disk ratio. Therefore, while radionuclides can explain the observed disk emission, an additional positron source seems necessary to explain the bulge emission.<sup>1</sup> We are therefore motivated to explore alternative proposals for the source of the bulge positrons, especially given the strong concentration of the signal in the inner bulge [23].

Although many DM models have been constructed to produce excess positrons through inelastic scattering followed by decay [22, 24–30], by direct decays of metastable DM [22, 25, 31], or by direct annihilation of MeV-scale DM [32–34], it is important to note whether such models can be tested (and potentially excluded) through complementary experiments. Connecting to direct detection of the DM is clearly interesting for any such scenario. But in hidden sector models, the new particles that mediate the DM interactions can also be discoverable in beam dump experiments. Moreover if the mediator is a scalar that mixes with the standard model (SM) Higgs boson, then new signatures can arise in rare decays involving the scalar. Of the three classes of models mentioned above, decaying DM is ruled out as a source of galactic 511 keV gamma rays because it predicts a much broader spatial distribution than is observed [35, 36]. Inelastic scattering to excited dark matter (XDM) on the other hand gives a very good fit to the observed shape [23]. In addition, the mass scale of XDM is not restricted, since it only requires that the mass splitting between nearby states, not the masses themselves, be at the MeV scale. This affords stronger possibilities for such DM to be discovered in existing or imminent direct detection experiments.

In the present work, we propose a new class of XDM models, guided by the desire for simplicity and for complementary signals in a range of experiments, which may exclude or constrain these models. Many of the recent XDM models were based upon exchange of hidden sector nonabelian gauge bosons [22, 26, 28, 37]. In the present work we aim to build the minimal XDM model based upon an Abelian gauge symmetry. It will be seen that these models are not as economical as the original XDM model proposed in [24], which relied upon scalar boson exchange. The main reason for additional complications in the case of gauge boson exchange is that DM scatterings must be inelastic at *both* interaction vertices, whereas with scalar exchange, it is possible to have elastic scattering at one vertex. The result is that gauge models necessarily produce two  $e^+e^-$  pairs, which is energetically more difficult than making just a single pair, and suppresses the rate of positron production since one relies upon the tail of the DM velocity distribution to have enough kinetic energy to produce the pairs. While it is possible to achieve the observed rate in the galactic

---

<sup>1</sup> To quote ref. [20]: “However, in view of the different conditions—density, magnetic field and unknown level of small-scale turbulence—in the Bulge, such a calculation [that of ref. [17]] appears rather arbitrary (although not necessarily wrong). Their model can be considered as a quantitative illustration of a possible scenario, the plausibility of which remains to be shown.” The criticisms of ref. [21] are more pointed: “[The authors of ref. [17]] claim that differential propagation of nucleosynthesis positrons can explain all properties of the INTEGRAL/SPI observations. We reach a different conclusion, at least for the morphology of the annihilation emission. We identified several [four] assumptions in the work of [ref. [17]] that may explain the discrepancy and review them in the following. . .” Detailed criticisms of the claims in [18] that dark matter annihilation cannot explain the observed signal are also given in section V.D of [22].

center with scalar models having only two dark matter states [30], it is much more difficult to do so in gauge boson models [29]. To overcome this difficulty, it was proposed to have three states of DM, one of which is metastable and having a smaller energy gap to its neighboring state than  $2m_e$  [28]. The smaller gap allows for a larger rate of excitation, or de-excitation in case the metastable state is the heaviest of the three [22]. Because of this need for three DM states, our present model requires three Weyl DM particles, and a kinetically mixed U(1) gauge boson. It also requires two new dark scalars, one real and one complex. Despite the many free parameters, we will show that the model is highly constrained and allows for a number of complementary experimental tests. In contrast, the much simpler model of [24] does not seem to offer any additional tests that would facilitate its exclusion (or provide hints toward its confirmation).

Our analysis is similar to that in ref. [22], except that the latter considered nonabelian DM which required rather elaborate Higgs sectors and hierarchies of gauge kinetic mixing in order to get the desired mass splittings and lifetime of the metastable DM state. The model presented here is simpler. We also employ improvements in direct detection limits from XENON100 and updated analyses of the CoGeNT signals relative to what existed at the time of ref. [22].

## 2 Defining the model

The minimal models for XDM consist of three Weyl fermions as the DM states.<sup>2</sup> Since the top two are nearly degenerate, it is natural to consider them as being originally the components of a Dirac fermion, split by some small symmetry breaking due to a hidden sector complex Higgs  $\phi$ ; after symmetry breaking, the DM is a triplet of Majorana fermions  $\chi_{1,2,3}$ . As in [22], the mass splitting  $\delta M_{12}$  between the lowest and two highest states must be accidentally of order a few MeV, while the smaller splitting  $\delta M_{23}$  between the two highest states appears naturally due to the underlying symmetry. We will also require an additional real singlet  $\Phi$  in order to get the correct relic density for the DM ground state  $\chi_1$ .

We denote the three Weyl states in the Lagrangian basis by  $\psi_1, \psi_2, s$ , with charges  $+1, -1, 0$  respectively under the dark gauged U(1). Let the scalars  $\phi$  and  $\Phi$  have charge  $-1$  and  $0$  respectively. Omitting for now the Higgs potential terms, this gives rise to the Lagrangian

$$\mathcal{L} = M_\chi \psi_1 \psi_2 + \frac{1}{2}(m + y_\Phi \Phi)ss + (y_1 \phi \psi_1 s + y_2 \phi^* \psi_2 s + \text{h.c.}) + g Z'_\mu (\psi_1^\dagger \sigma^\mu \psi_1 - \psi_2^\dagger \sigma^\mu \psi_2) \quad (1)$$

where  $Z'$  is the new U(1) gauge boson, and we use the shorthand  $\psi_1 \psi_2 = \psi_1^T \sigma_2 \psi_2$  for the Lorentz invariant spin contractions. The  $Z'$  is assumed to kinetically mix with the photon (properly hypercharge), and the two scalars will acquire some small mixing with the SM Higgs  $H$ , by virtue of Higgs portal terms  $|H|^2 |\phi|^2$  and  $|H|^2 \Phi^2$  and nonvanishing VEVs for  $\phi$  and  $\Phi$ . Furthermore,  $\phi$  and  $\Phi$  can mix with each other after symmetry breaking through  $|\phi|^2 \Phi^2$ ; for simplicity, we will assume that this mixing angle is negligible in the following. For notational convenience, we henceforth absorb  $y_\Phi \langle \Phi \rangle$  into the definition of  $m$ .

Suppose that the masses are such that  $M_\chi - m \gtrsim 2m_e$ <sup>3</sup> (and provisionally  $m, M_\chi \sim 10$  GeV to eventually make contact with direct detection experiments), so that before  $\phi$  gets a VEV, we have a Dirac state with slightly higher mass than that of  $s$ . When  $\phi$  gets its VEV, this splits into two nearby Majorana states with masses

$$M_+ = M_\chi + \frac{(\mu_1 + \mu_2)^2}{2(M_\chi - m)}, \quad M_- = M_\chi + \frac{(\mu_1 - \mu_2)^2}{2(M_\chi + m)} \quad (2)$$

<sup>2</sup> We prefer fermions to scalars for the DM because the small masses and mass splittings of fermions are stable under renormalization.

<sup>3</sup> Only rarely do the positrons pair-annihilate in flight (they must first form positronium), so the  $e^+$  injection energy, which is of order  $M_\chi - m \gtrsim 2m_e$ , must be  $\lesssim 10$  MeV; see, for example, [20].

where  $\mu_i \equiv y_i \langle \phi \rangle$ . Presently, we will argue for a symmetry that imposes  $\mu_1 + \mu_2 = 0$ . Then we can use the seesaw mechanism to explain the smaller of the two mass splittings so long as  $\mu_i \ll (M_\chi + m)$ . For example if  $\mu_i \sim 10$  MeV, then we get  $\delta M_{23} \sim 10$  keV which is the desired scale indicated by our earlier study of a similar model in ref. [22].

We need to gauge the U(1) symmetry to get rid of the Goldstone boson that would arise from  $\phi$  getting its VEV; otherwise the massless boson could mediate problematic long-range forces coupling to the dark matter. This is the origin of the dark gauge boson  $Z'$ . Notice that with our choice of charges the model is anomaly free. In the limit of vanishing gauge kinetic mixing,  $\epsilon \rightarrow 0$ , this is obvious because  $Z'$  couples only to a Dirac fermion  $\psi$ . Nonvanishing  $\epsilon$  can be induced for example by integrating out a heavy scalar that carries both the dark U(1) and weak hypercharge, which cannot induce any anomaly. Ignoring the  $Z$  boson, the gauge kinetic mixing term is

$$-\frac{\epsilon}{2} F^{\mu\nu} Z'_{\mu\nu} \quad (3)$$

where  $F_{\mu\nu}$  is the electromagnetic field strength and  $Z'_{\mu\nu}$  is that of the dark U(1). After diagonalization of the kinetic term,  $Z'$  acquires a coupling to the electromagnetic current with the extra  $\epsilon$  suppression factor. This allows  $Z'$  to mediate the decay  $\chi_2 \rightarrow \chi_1 e^+ e^-$ .

One of the challenges for this model is that the rates of decay of the mass eigenstates  $\chi_2 \rightarrow \chi_1 e^+ e^-$  and  $\chi_3 \rightarrow \chi_1 e^+ e^-$  must be quite different from each other in order for  $\chi_3$  to be cosmologically long-lived while  $\chi_2$  decays relatively promptly. This difference can be naturally realized by invoking a discrete symmetry  $\psi_1 \leftrightarrow \psi_2$ ,  $\phi \leftrightarrow -\phi^*$  that insures that  $y \equiv y_1 = -y_2$  hence  $\mu_1 = -\mu_2$ . In this case we obtain distinctly different couplings between the two highest mass eigenstates and the lowest one. The relation between the flavor states and the mass states is approximately

$$\psi_1 \simeq \frac{1}{\sqrt{2}}(\chi_2 + \chi_3 + \eta\chi_1), \quad \psi_2 \simeq \frac{1}{\sqrt{2}}(\chi_2 - \chi_3 - \eta\chi_1), \quad s \simeq \chi_1 - \eta\chi_3, \quad (4)$$

where  $\eta \equiv \sqrt{2}y\langle\phi\rangle/(M_\chi + m)$  is the small mixing parameter between the  $\psi$  and  $s$  sectors. The mass splitting between the top two states is  $\delta M_{23} = \eta^2(M_\chi + m)$ . With the above choices, we obtain different kinds of couplings between  $\chi_1$ - $\chi_2$  and  $\chi_1$ - $\chi_3$ ,

$$\mathcal{L}_{\text{int}} = y\phi [\chi_3\chi_1 + \eta(\chi_1^2 - \chi_3^2)] + \frac{1}{2}y_\Phi\Phi [\chi_1^2 - \eta(\chi_1\chi_3 + \chi_3\chi_1)] + \chi_2^\dagger g Z'_\mu \sigma^\mu (\chi_3 + \eta\chi_1) + \text{h.c.} \quad (5)$$

where now  $\phi$  stands for the canonically normalized real part of the complex scalar. This allows us to create a natural hierarchy between the  $\chi_2$  and  $\chi_3$  lifetimes. The decay  $\chi_3 \rightarrow \chi_1 e^+ e^-$  is mediated only by  $\phi$ , and that of  $\chi_2 \rightarrow \chi_1 e^+ e^-$  proceeds by the  $Z'$ . In terms of 4-component Majorana spinors  $\chi_{1,2,3}$ , the Yukawa and gauge couplings become

$$\mathcal{L}_{\text{int}} = y\phi [\bar{\chi}_3\chi_1 + \eta(\bar{\chi}_1\chi_1 - \bar{\chi}_3\chi_3)] + y_\Phi\Phi (\bar{\chi}_1\chi_1 - \eta\bar{\chi}_1\chi_3) + g\bar{\chi}_2\cancel{Z}'(\chi_3 + \eta\chi_1). \quad (6)$$

The mass spectrum and the different kinds of transitions between the states are depicted qualitatively in fig. 1. The model is necessarily *exothermic*: the heaviest state  $\chi_3$  is the one that can be made metastable on time scales greater than the age of the universe. Thus the process  $\chi_3\chi_3 \rightarrow \chi_2\chi_2$ , that leads to fast  $\chi_2 \rightarrow \chi_1 e^+ e^-$  decays at the galactic center, is not impeded by any energy barrier.

### 3 The 511 keV signal and relic density

In this section, we will discuss requirements on the couplings of our model to account for both the DM relic abundance and the 511 keV signal from the galactic center. These are the two major constraints on any XDM model which must be satisfied.<sup>4</sup> We consider them in turn.

<sup>4</sup> Another possibility, which we do not consider here, is to get the 511 keV signal from a subdominant component of dark matter whose excitation cross section is correspondingly larger.

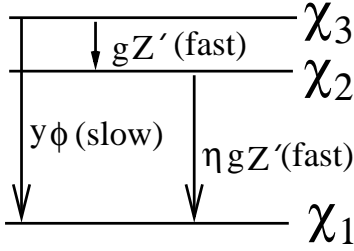


**Fig. 1** Schematic depiction of DM mass spectrum and the transitions between the states. The  $\chi_3 \rightarrow \chi_1 e^+ e^-$  transition is a very slow decay mediated by  $\phi$ , while  $\chi_3 \chi_3 \rightarrow \chi_2 \chi_2$  is a fast annihilation process and  $\chi_2 \rightarrow \chi_1 e^+ e^-$  is a fast decay mediated by  $Z'$ .

### 3.1 Scattering rate for $e^+$ production

The cross section for  $\chi_3 \chi_3 \rightarrow \chi_2 \chi_2$  is given in eq. (36) of ref. [22]. For the parameter values of interest here, it simplifies to

$$\sigma_{\downarrow} v_{\text{rel}} = \frac{g^4 M_{\chi}^2}{4\pi m_{Z'}^4} \sqrt{v^2 + v_t^2}, \quad (7)$$

where the  $v_t$  denotes the threshold velocity for the *inverse* reaction  $\chi_2 \chi_2 \rightarrow \chi_3 \chi_3$  in the center-of-mass frame:  $v_t = \sqrt{2\delta M_{23}/M_{\chi}}$ . The rate of scatterings in the galactic center is given by eq. (28) of the same reference:  $R_{e^+} = 2 \times \frac{1}{2} (Y_3/Y_{\text{tot}})^2 \int d^3x \langle \sigma_{\downarrow} v_{\text{rel}} \rangle (\rho/M_{\chi})^2$ , where  $Y_3/Y_{\text{tot}}$  is the relative abundance of  $\chi_3$ ,  $\rho$  is the DM mass density, and the integral is taken over radii corresponding to the INTEGRAL observations,  $r \lesssim r_c \equiv 1.5$  kpc (the first factor of 2 accounts for the fact that each scattering produces two  $e^+e^-$  pairs). One must perform the phase space average over the DM velocity distribution to compute  $\langle \sigma_{\downarrow} v_{\text{rel}} \rangle$ , which depends upon  $r$  because the mean and escape velocities of the DM are  $r$ -dependent. We have carried out these integrations numerically for a range of different DM density profiles, assumed to be Einasto profiles  $\rho = \rho_{\odot} \exp(-(2/\alpha)((r/r_s)^{\alpha} - (r_{\odot}/r_s)^{\alpha}))$  with  $\rho_{\odot} = 0.3$  GeV/cm<sup>3</sup>. In this way we can express the rate of positron production in the form

$$R_{e^+} = 4\pi \zeta_{\downarrow} v_t \frac{\rho_{\odot}^2}{M_{\chi}^2} \left( \frac{Y_3}{Y_{\text{tot}}} \right)^2 \overline{\sigma v} \times (1 \text{ kpc})^3 \quad (8)$$

where  $\overline{\sigma v} = g^4 M_{\chi}^2 / 4\pi m_{Z'}^4$ , and

$$\zeta_{\downarrow} = \text{kpc}^{-3} \int_0^{r_c} dr r^2 (\rho/\rho_{\odot})^2 \left\langle \sqrt{v^2/v_t^2 + 1} \right\rangle. \quad (9)$$

We have used the same velocity distribution function as described in [22] for the phase-space average, and assumed that  $v_t = 2\eta = \sqrt{2 \times 10^{-6}}$ , corresponding to  $\delta M_{23} = 10$  keV,  $M_{\chi} = 10$  GeV. The numerical results for  $\zeta_{\downarrow}$  are shown in fig. 2. Equating (8) to the observed rate of  $1.1 \times 10^{43} \text{ s}^{-1}$  gives the constraint

$$\frac{m_{Z'}}{g} = 6.5 \text{ GeV} \left( \frac{\zeta_{\downarrow}}{3000} \right)^{1/4} \left( \frac{\eta}{10^{-3}} \right)^{1/4} \left( \frac{\bar{Y}}{0.33} \right)^{1/2}, \quad (10)$$

where we defined  $\bar{Y} = Y_3/Y_{\text{tot}}$ . We note that for DM halo profiles close to those found in N-body simulations for Milky Way-like galaxies,  $\zeta_{\downarrow} \sim 3000$ , leading to the restriction that  $m_{Z'} \lesssim 20$  GeV to keep the coupling  $g$  perturbative ( $g \lesssim \sqrt{4\pi}$ ). We find that the contours of  $\zeta_{\downarrow}$  shift very little for values of  $v_t = 2\eta$  larger than the assumed  $1.4 \times 10^{-3}$ , but they start to shift noticeably to the right for smaller values.

The total positron production rate within the bulge is, of course, not the only observable characterizing the 511 keV gamma ray signal. As has been stressed in [23, 35, 36], the gamma ray intensity is strongly peaked near the galactic center, with a best fit similar to  $\rho(r)^2$  for an

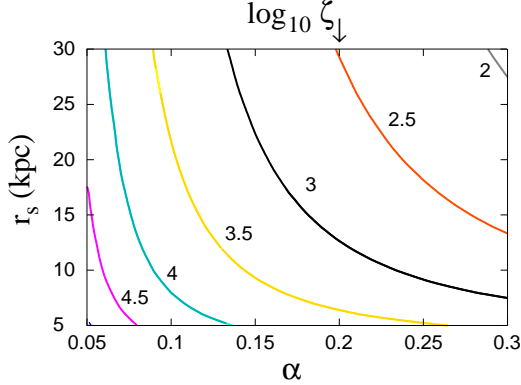


**Fig. 2** Contours of the log of  $\zeta_{\downarrow}$ , defined in (9), as a function of Einasto halo profile parameters  $\alpha$  and  $r_s$ . The threshold velocity  $v_t = 1.4 \times 10^{-3}$  is assumed.

Einasto profile with  $\alpha = 0.17$ ,  $r_s = 26$  kpc [23]. While it is possible that positrons from outside the center of the galaxy propagate toward the center to annihilate [17, 18], it seems simpler to assume that the  $e^+$  sources are concentrated in the galactic center and that  $e^+$  do not propagate long distances before annihilating. In fact ref. [21] has recently argued that, while positrons may escape the galactic bulge or disk in some propagation models, those which annihilate tend to do so near their sources, at least for positrons that are injected with only several hundred keV of kinetic energy. It therefore seems reasonable to assume that the positrons do not travel very far before annihilating.

### 3.2 Relic density

The requirement of getting the right DM relic density through thermal decoupling significantly restricts the parameters of the model. We start with a summary of the key considerations. As we will show in section 4.2, the  $\chi_1$  and  $\chi_{2,3}$  states do not scatter efficiently into each other after the DM species freeze out chemically, and scatterings of  $\chi_{2,3}$  into each other freeze out before  $\chi_3$  is significantly depleted. As a result, chemical freezeout determines both the total DM relic density and the relative abundance  $Y_3$  of the metastable DM state. Moreover we will show that at the time of chemical freezeout,  $\chi_2$  and  $\chi_3$  have the same abundance; in order for them to be the main components of the DM, we require the abundance of  $\chi_1$  to be subdominant. However  $\chi_1$  couples too weakly to  $Z'$  and  $\phi$  to efficiently annihilate, so we take advantage of the singlet Higgs  $\Phi$  to dilute it through  $\chi_1\chi_1 \rightarrow \Phi\Phi$ . On the other hand,  $\chi_2$  and  $\chi_3$  have an unsuppressed coupling to  $Z'$ , so the gauge interactions dominate their annihilation cross sections and determine their relic density. A summary of the values of the couplings and masses needed to satisfy these restrictions (as well as others to be discussed below) is provided in table 1. Typically the scalars  $\phi, \Phi$  must be somewhat lighter than the DM, while the  $Z'$  may be lighter or more massive.

We consider first the total relic abundance of  $\chi_{2,3}$ , which is determined by the dark gauge interactions. The strongest annihilation channels available are  $\chi_2\chi_2 \rightarrow Z'Z'$ ,  $\chi_3\chi_3 \rightarrow Z'Z'$  and  $\chi_2\chi_3 \rightarrow f\bar{f}$  where  $f$  is a SM fermion.  $\chi_2$  and  $\chi_3$  can also annihilate into the scalars  $\phi, \Phi$ , but the relevant couplings are suppressed, so we can ignore these channels. The average annihilation cross section for  $\chi_2\chi_2$ ,  $\chi_2\chi_3$ ,  $\chi_3\chi_3$ , including the annihilations into  $Z'$  and co-annihilations into SM fermions, is given by

$$\langle\sigma_{\text{ann}}v\rangle = \frac{1}{32\pi M_\chi^2} S(g, \epsilon, m_{Z'}/M_\chi) , \quad (11)$$

where

$$S(g, \epsilon, x) = \frac{1}{2} g^4 f_1(x) + (g\epsilon e)^2 \sum_i N_{c,i} Q_i^2 f_2(x, x_i) , \quad (12)$$

Parameter	Scaling	Fiducial Value
$M_\chi$	independent	10 GeV
$\eta$	..	$10^{-3}$
$\zeta_\downarrow$	..	3000
$\epsilon$	..	$\gtrsim 10^{-6}$
$\mu_\Phi \sim m_\Phi$	constrained	$\gtrsim 5$ GeV
$y_\Phi$	..	$\lesssim 1/10$
$\Theta$	..	$\lesssim 6 \times 10^{-4}$
$m_\phi \sim \langle \phi \rangle$	$(\zeta_\downarrow \eta)^{1/4} \bar{Y}^{1/2}$	4.6 GeV
$y$	$M_\chi \eta^{3/4} \zeta_\downarrow^{-1/4} \bar{Y}^{-1/2}$	$3 \times 10^{-3}$
$\theta$	$(M_\chi / \bar{Y})^{1/2}$	$\lesssim 10^{-5}$
$m_{Z'} (\chi\chi \rightarrow Z'Z')$	$(\zeta_\downarrow \eta \bar{Y})^{1/4} M_\chi^{1/2}$	610 MeV
$g$	$M_\chi^{1/2} \bar{Y}^{-1/4}$	0.094
$m_{Z'} (\chi\chi \rightarrow ff)$	$M_\chi$	20 GeV
$g$	$M_\chi (\zeta_\downarrow \eta)^{-1/4} \bar{Y}^{-1/2}$	3.08

**Table 1** Model parameters and their fiducial values. The second column shows how the fiducial value of the dependent parameters scales with the values of independent ones.  $m_{Z'}$  and  $g$  are given for two possible dominant annihilation channels.

with the sum over all kinematically allowed SM fermions having charge  $Q_i$  and number of colors  $N_{c,i}$ . The kinematic functions are given by  $f_1 = (1 - x^2)^{3/2} / (1 - \frac{1}{2}x^2)^2 \Theta(1 - x)$  and  $f_2(x, x_i) = (1 + \frac{1}{2}x_i^2) (1 - x_i^2)^{1/2} / (1 - \frac{1}{4}x^2)^2 \Theta(1 - x_i)$ , where  $x_i = m_i/M_\chi$ . This cross section controls the total abundance of  $\chi_2$  and  $\chi_3$ . To analyze this, we eliminate  $g$  in favor of  $m_{Z'}$  using (10) and taking our canonical values for  $\eta$ ,  $\zeta_\downarrow$ ,  $\bar{Y}$  (see table 1). For several values of  $\epsilon$ , we determine contours in the plane of  $M_\chi$ - $m_{Z'}$  that give the required cross section,  $\langle \sigma_{\text{ann}} v \rangle = (2\bar{Y})^{-1} \times 3 \times 10^{-26} \text{ cm}^3/\text{s}$ . The factor of  $2\bar{Y}$  reduces the relative abundance of  $\chi_3$  to  $\bar{Y}$ , with the same relative abundance for  $\chi_2$  at freezeout (since annihilations of  $\chi_2$  have the same cross section as annihilations of  $\chi_3$ ); at generic points in the allowed parameter space, there is no kinetic equilibrium after freeze-out, so the present-day value is the same as that at the freeze-out temperature,  $\bar{Y}_0 = \bar{Y}(T_f)$ . (More quantitatively, the required cross section is reduced slightly due to the presence of extra light degrees of freedom; see, for example, the discussion of [22].)

The resulting possible relations between  $M_\chi$  and  $m_{Z'}$  giving the observed relic density are shown in fig. 3, for several values of the gauge kinetic mixing parameter  $\epsilon$ . For any value of  $\epsilon$ , there are always two solutions in which the  $g^4$  contribution to  $\sigma_{\text{ann}}$  dominates. The lower branch has

$$\begin{aligned}
m_{Z'} &= (610 \text{ MeV}) \times \left( \frac{M_\chi}{10 \text{ GeV}} \right)^{1/2} \left( \frac{\zeta_\downarrow}{3000} \right)^{1/4} \left( \frac{\eta}{10^{-3}} \right)^{1/4} \left( \frac{\bar{Y}}{0.33} \right)^{1/4} \\
g &= 0.094 \left( \frac{M_\chi}{10 \text{ GeV}} \right)^{1/2} \left( \frac{\bar{Y}}{0.33} \right)^{-1/4}.
\end{aligned} \tag{13}$$

The upper branch is the unlikely situation in which  $g$  would be too large to give the right relic density, but  $m_{Z'} \simeq M_\chi$  so that the phase space nearly vanishes; we will not explore this case. There are also solutions where annihilation to SM fermions dominates at  $m_{Z'} > M_\chi$ . These contours depend somewhat on the value of  $\epsilon$ ,  $\eta$ , and  $\zeta_\downarrow$ , but they are centered around the condition for resonance in the  $s$ -channel,

$$\begin{aligned}
m_{Z'} &\simeq 2M_\chi \\
g &\simeq 3.08 \left( \frac{M_\chi}{10 \text{ GeV}} \right) \left( \frac{\zeta_\downarrow}{3000} \right)^{-1/4} \left( \frac{\eta}{10^{-3}} \right)^{-1/4} \left( \frac{\bar{Y}}{0.33} \right)^{-1/2}.
\end{aligned} \tag{14}$$

The gauge coupling tends to be nonperturbatively large on this branch, unless  $M_\chi$  is significantly smaller than 10 GeV.



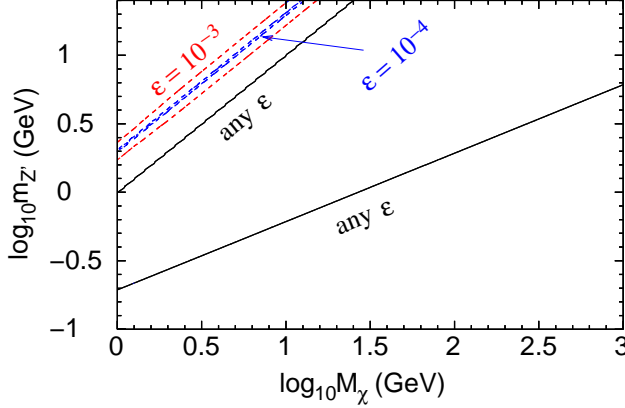


**Fig. 3** Contours corresponding to the observed relic density for  $\chi_{2,3}$  in the  $M_\chi$ - $m_{Z'}$  plane, assuming the relation (10) and  $\zeta_\downarrow = 3000$ . Lowest two curves (solid) are due to  $\chi\chi \rightarrow Z'Z'$ , while higher ones (dashed) are due to  $\chi\chi \rightarrow f\bar{f}$ .

In the case that  $\chi\chi \rightarrow Z'Z'$  determines the  $\chi_{2,3}$  abundance, it is worth noting that  $\chi_2$ ,  $\chi_3$ , and  $Z'$  were in equilibrium with the SM until the time of freeze-out, so that the standard estimate of their relic abundance applies. To see this, consider the Compton-like scattering  $Z'f \rightarrow \gamma f$  ( $Z'\gamma \rightarrow f\bar{f}$  pair production has a similar cross section), where  $f$  is a relativistic SM fermion; at the temperatures when  $\chi_{2,3}$  freeze out, these are  $e, \mu, u, d, s$ . Ignoring all particle masses for simplicity and using  $3T$  as an estimate for typical energies and momenta, we estimate the cross section for this scattering as

$$\langle \sigma_{Z'f \rightarrow \gamma f v} \rangle \approx \frac{\pi Q_i^4 \alpha^2 \epsilon^2}{18T^2}. \quad (15)$$

If we sum over all the available fermion species (including colors), the rate per  $Z'$  to scatter into  $\gamma$  is larger than  $3H$  at  $T \approx 500$  MeV for  $\epsilon \gtrsim 3 \times 10^{-7}$ . As we will see in section 4.1 below,  $\epsilon$  must be larger than this value for  $\chi_2$  to decay quickly enough. In fact, we have checked in detail (including all particle masses and appropriate thermal averages) that this scattering remains in equilibrium down to temperatures of about the electron mass for  $\epsilon \gtrsim 10^{-6}$ . Therefore, the dark sector remains in equilibrium with the SM through  $\chi_{2,3}$  freezeout.

For the relic density of  $\chi_1$ , the coannihilation  $\chi_1\chi_2 \rightarrow Z'Z'$  has an amplitude suppressed by  $\eta \sim 10^{-3}$ , so there must exist other annihilation channels to prevent  $\chi_1$  from dominating the DM density and thereby diluting the contribution of  $\chi_3$  to the 511 keV signal. Similarly, as will be shown in sections 3.3 and 4, annihilations to  $\phi$  are suppressed by the small Yukawa coupling  $y$ . If the real singlet  $\Phi$  is light however, we can consider  $\chi_1\chi_1 \rightarrow \Phi\Phi$  annihilations. (There are also annihilations  $\chi_1\chi_1 \rightarrow f\bar{f}$  to light SM fermions by  $s$ -channel boson exchange, but this is greatly suppressed by the small SM Yukawa couplings and  $\Phi$ -Higgs mixing angle.) Annihilation to  $2\Phi$  proceeds by  $s, t, u$  channels with a trilinear  $\Phi$  coupling  $\mu_\Phi$  in the  $s$  channel, and the cross section is  $p$ -wave suppressed. When the  $s$ -channel dominates,

$$\sigma v_{\text{rel}} \approx \frac{\mu_\Phi^2 y_\Phi^2}{512\pi M_\chi^4} v^2 \frac{\sqrt{1-x^2}}{(1-x^2/4)^2}, \quad x = m_\Phi/M_\chi. \quad (16)$$

Assuming that freezeout occurs at  $T \sim M_\chi/18$  (as is appropriate for DM with mass  $\sim 10$  GeV) and demanding that  $\langle \sigma_{\text{ann}} v \rangle = 3 \times 10^{-26} Y_{\text{tot}}/Y_1 \text{ cm}^3/\text{s}$  to obtain  $\chi_1$  relic abundance  $Y_1 < Y_{\text{tot}}$  leads to the constraint

$$\mu_\Phi \simeq \frac{0.15}{y_\Phi} \left( \frac{Y_{\text{tot}}}{Y_1} \right)^{1/2} \left( \frac{M_\chi}{10 \text{ GeV}} \right)^2 \text{ GeV}, \quad (17)$$

where we have assumed that the kinematic  $x$ -dependent factors are order unity. We can achieve an acceptable abundance,  $Y_1/Y_{\text{tot}} = 0.006$  for example, with reasonable parameter choices like



$y_\Phi = 0.1$ ,  $\mu_\Phi \simeq m_\Phi \simeq 5$  GeV. This relationship could also hold for annihilation  $\chi_1\chi_1 \rightarrow \phi\phi$  if  $\mu_\Phi$  is the coupling for  $\Phi|\phi|^2$ .

We note that the value of  $Y_1$  at freezeout is not the same as its present-day value;  $\chi_2 \rightarrow \chi_1 e^+ e^-$  decays will enhance  $Y_1$  nonthermally, as the rate of this decay is generically much slower than the Hubble rate at chemical freezeout. Since only  $\chi_3$  participates in  $e^+$  production and direct detection and  $Y_3$  is fixed after chemical freezeout, we are not concerned with the present-day value of  $Y_1$ .

### 3.3 Relations between model parameters

In addition to the relationships between model parameters required for the observed relic density and galactic positron production, there are several others.

The complex scalar vacuum expectation value and  $Z'$  mass satisfy

$$\frac{1}{2}m_{Z'}^2 \leq g^2 \langle \phi \rangle^2, \quad (18)$$

where the inequality is saturated when there is no other scalar whose VEV breaks the dark U(1) to give mass to the  $Z'$ . Making this assumption, (10) implies that

$$\langle \phi \rangle = 4.6 \text{ GeV} \left( \frac{\zeta_\downarrow}{3000} \right)^{1/4} \left( \frac{\eta}{10^{-3}} \right)^{1/4} \left( \frac{\bar{Y}}{0.33} \right)^{1/2}. \quad (19)$$

For standard scalar potentials with dimensionless couplings no greater than  $\mathcal{O}(1)$ ,  $m_\phi \lesssim \langle \phi \rangle$ , so we can infer an upper limit on the mass of  $\phi$ . Moreover, the definition of the mixing parameter  $\eta$  gives

$$y \simeq \frac{\sqrt{2}\eta M_\chi}{\langle \phi \rangle} = 3.0 \times 10^{-3} \left( \frac{M_\chi}{10 \text{ GeV}} \right) \left( \frac{\zeta_\downarrow}{3000} \right)^{-1/4} \left( \frac{\eta}{10^{-3}} \right)^{3/4} \left( \frac{\bar{Y}}{0.33} \right)^{-1/2}. \quad (20)$$

Table 1 summarizes the values of  $\langle \phi \rangle$ ,  $y$ ,  $m_{Z'}$ , and  $g$  in terms of the other model parameters. We take as fiducial values  $M_\chi = 10$  GeV,  $\zeta_\downarrow = 3000$ ,  $\eta = 10^{-3}$ , and  $\bar{Y} = 1/3$ . These are further supplemented by (10) relating  $m_{Z'}$  and  $g$  and (17) for the cubic coupling of the neutral scalar  $\Phi$ .

## 4 Other constraints

Besides the relic density and rate of galactic positron production, we need to insure that the metastable state  $\chi_3$  is sufficiently long-lived and that it is not depleted by  $\chi_3\chi_3 \rightarrow \chi_2\chi_2$  down-scattering in the early universe.

### 4.1 Lifetimes of excited states

A necessary condition for our exothermic XDM model is that the excited state  $\chi_3$  must be long-lived compared to the age of the universe. In fact, the rate of  $\chi_3 \rightarrow \chi_1 e^+ e^-$  decays must be significantly less than that of  $\chi_3\chi_3 \rightarrow \chi_2\chi_2$  downscatterings to insure that the 511 keV signal has the right morphology, proportional to the DM density profile squared,  $\rho(r)^2$ , rather than  $\rho(r)$ .

The  $\chi_2$  state on the other hand must decay relatively quickly via  $\chi_2 \rightarrow \chi_1 e^+ e^-$ , mediated by  $Z'$  exchange. Let us consider it first. From eq. (50) of [22], the rate is given by

$$\Gamma_2 = 2\alpha_g \alpha \epsilon^2 \eta^2 m_e^2 (\delta M_\chi - 2m_e)^3 m_{Z'}^{-4} \simeq \frac{\alpha g^2 \epsilon^2 \eta^2 m_e^5}{2\pi m_{Z'}^4}, \quad (21)$$

where  $\alpha$  is the fine structure constant,  $\alpha_g = g^2/4\pi$ , and  $\epsilon$  is the kinetic mixing parameter between  $Z'$  and the photon. We have assumed that  $\delta M_\chi - 2m_e \sim m_e$  in the absence of fine tuning.

$\tau_2 = 1/\Gamma_2$  should be small compared to the time it takes a  $\chi_2$  DM particle to travel  $\sim 1$  kpc at the typical speed of  $10^{-3}c$ . Otherwise the signal will become spatially more spread-out than observed due to the propagation of  $\chi_2$ . This gives the constraint

$$\frac{\sqrt{\eta g \epsilon \epsilon}}{m_{Z'}} \gg \frac{1}{82 \text{ TeV}}, \quad (22)$$

which is easily satisfied. For example using  $\eta = 10^{-3}$ ,  $M_\chi = 10$  GeV,  $m_{Z'} = 600$  MeV,  $g = 0.09$  (see eq. (13)), we find  $\epsilon \gg 1.6 \times 10^{-6}$ .

The decay  $\chi_3 \rightarrow \chi_1 e^+ e^-$  is mediated by the  $\phi$  and  $\Phi$  mixing with the SM Higgs. The matrix element is the same as in the vector-mediated case except that both  $\phi$  and  $h$  contribute, leading to a decay rate

$$\Gamma_3 = \frac{\alpha_{y_e} m_e^2 (\delta M_\chi - 2m_e)^3}{2\pi} \left[ \frac{y c_\theta s_\theta}{m_\phi^2} - \frac{y_\Phi \eta c_\Theta s_\Theta}{m_\Phi^2} + \frac{y_\Phi \eta c_\Theta s_\Theta - y c_\theta s_\theta}{m_h^2} \right]^2, \quad (23)$$

where  $\alpha_{y_e} = m_e^2/4\pi v^2$ ,  $v = 246$  GeV is the Higgs VEV, and  $\theta, \Theta$  are the  $\phi$ -Higgs and  $\Phi$ -Higgs mixing angles respectively. In the absence of finely-tuned destructive interference between the Yukawa couplings and mixing angles, we find

$$\Gamma_3 \simeq \max \left( \frac{y^2 \theta^2 m_e^7}{8\pi^2 M_\phi^4 v^2}, \frac{y_\Phi^2 \eta^2 \Theta^2 m_e^7}{8\pi^2 M_\Phi^4 v^2} \right). \quad (24)$$

Here we have assumed that  $\theta, \Theta \ll 1$  and denoted  $M_{\phi, \Phi}^4 = (m_h^{-2} - m_{\phi, \Phi}^{-2})^{-2}$ . (Notice that  $M_{\phi, \Phi}$  is approximately given by  $\min(m_{\phi, \Phi}, m_h)$  if the dark scalar masses are not close to that of the SM Higgs.) Small values of  $\theta, \Theta$  are clearly preferred for suppressing  $\Gamma_3$ .

Comparing to the observed rate of positron emission in the galactic center, eq. (38) of [22], we can constrain the couplings in terms of the other model parameters. Demanding that  $\Gamma_3$  be sufficiently small, so that downscatterings dominate over decays to produce the observed positrons, we find (in the case where  $\phi$  exchange dominates the decay of  $\chi_3$ )

$$y^2 < \left( \frac{0.33}{\bar{Y}} \right) \left( \frac{25}{\zeta} \right) \left( \frac{\delta M_\chi}{m_e} - 2 \right)^{-3} \left( \frac{10^{-2}}{\theta} \right)^2 \frac{M_\phi^4 M_\chi}{(600.3 \text{ GeV})^5} \quad (25)$$

where  $\zeta$  is defined as  $\zeta = \text{kpc}^{-3} \int_0^{r_c} dr r^2 \rho(r) / \rho_\odot$  as in eq. (38) of [22] (recall that  $\bar{Y} = Y_3/Y_{\text{tot}}$  is the abundance of  $\chi_3$  relative to the total  $\chi$  number). An analogous bound applies when  $\Phi$  dominates in  $\chi_3$  decay. We thus infer that

$$\max \left( \frac{\sqrt{y\theta}}{M_\phi}, \frac{\sqrt{y_\Phi \eta \Theta}}{M_\Phi} \right) < \frac{1}{19 \text{ TeV}} \left( \frac{M_\chi}{10 \text{ GeV}} \right)^{1/4} \left( \frac{\zeta}{25} \right)^{-1/4} \left( \frac{\bar{Y}}{0.33} \right)^{-1/4} \left( \frac{\delta M_\chi}{m_e} - 2 \right)^{-3/4}. \quad (26)$$

For example, with  $M_\phi \simeq m_\phi \simeq 4.6$  GeV and  $y = 3 \times 10^{-3}$  as in (19,20), the  $\phi$ - $H$  mixing angle must be very small,  $\theta \lesssim 2 \times 10^{-5}$ . The bound on  $y_\Phi \Theta$  is less stringent both due to the presence of  $\eta$  and the lack of an upper limit on  $m_\Phi$ . With  $m_\Phi \sim 5$  GeV,  $y_\Phi \sim 1/10$ , and  $\eta \sim 10^{-3}$ , we find  $\Theta \lesssim 6 \times 10^{-4}$ . We note that if  $m_\phi, m_\Phi \ll m_h$ , then a percent-level tuning of  $y\theta m_\phi^{-2} - y_\Phi \eta \Theta m_\Phi^{-2}$  can loosen these constraints significantly.

## 4.2 Washout of metastable states

In order for the relic density of the metastable state  $\chi_3$  to be relatively undepleted, we require that downscattering reactions capable of changing  $\chi_3$  number freeze out at temperatures above

the respective mass splitting  $\delta M_{23} \simeq 10$  keV or  $\delta M_{13} \simeq$  MeV. To be precise, these refer to the *kinetic* temperature of the  $\chi$  particles, which differs from the temperature of photons if the DM particles are no longer in kinetic equilibrium with the SM thermal bath.

We first consider kinetic equilibrium with the SM. The  $\chi_{2,3}$  population can be held in equilibrium with the SM by the single scattering process  $\chi_3 e \leftrightarrow \chi_2 e$ , which was considered for similar GeV-scale XDM in [22], with decoupling temperatures given in figure 11 of that reference.<sup>5</sup> For the preferred values of  $m_{Z'}, g, \epsilon$  given for direct detection in section 5 below, decoupling from the SM occurs at  $T_d = 36$  MeV; however, as indicated in section 5, scenarios with larger values of  $\epsilon$  and therefore lower  $T_d$  are possible. Since the kinetic temperature is  $T_k = T^2/T_d$  for SM temperature  $T$ , we have  $T_k = \delta M_{13}$  at  $T \sim 5 \delta M_{13}$  (assuming  $\delta M_{13} - 2m_e \sim m_e$ ) and  $T_k = \delta M_{23}$  at  $T \sim 60 \delta M_{23}$  (for  $\delta M_{23} \sim 10$  keV). The following constraints become less stringent if kinetic decoupling from the SM occurs later than 10 MeV temperatures.

Since we are concerned with the relic abundance of  $\chi_3$ , we need to ask which processes will change  $\chi_3$  number most efficiently. Besides scattering from electrons,  $\chi_3$  will be held in kinetic equilibrium by rapid  $\chi_3 \chi_3 \leftrightarrow \chi_2 \chi_2$  scattering mediated by  $Z'$ . The dominant scalar-mediated processes are  $\chi_3 \chi_3 \leftrightarrow \chi_1 \chi_1$  and  $\chi_3 \chi_1 \leftrightarrow \chi_1 \chi_1$ . There is no threshold velocity for downscattering, so the value of  $\langle \sigma_{\downarrow} v_{\text{rel}} \rangle$  at  $v = 0$  is the relevant one. For the three downscattering processes, these cross sections are

$$\begin{aligned} \langle \sigma_{33 \rightarrow 11} v_{\text{rel}} \rangle &= \frac{M_\chi^2}{4\pi} \left( \frac{y^2}{m_\phi^2} - \frac{y_\Phi^2 \eta^2}{m_\Phi^2} \right)^2 \sqrt{\frac{2\delta M_{13}}{M_\chi}}, \\ \langle \sigma_{31 \rightarrow 11} v_{\text{rel}} \rangle &= \frac{M_\chi^2}{4\pi} \left( \frac{y^2 \eta}{m_\phi^2} - \frac{y_\Phi^2 \eta}{m_\Phi^2} \right)^2 \sqrt{\frac{\delta M_{13}}{M_\chi}}, \\ \langle \sigma_{33 \rightarrow 22} v_{\text{rel}} \rangle &= \frac{M_\chi^2}{4\pi} \left( \frac{g}{m_{Z'}} \right)^4 \sqrt{\frac{2\delta M_{23}}{M_\chi}}. \end{aligned} \quad (27)$$

As throughout, we have assumed that the mediator masses satisfy  $m^2 \gg M_\chi \delta M$  for the mass splitting of each process above. We have ignored the  $s$ -channel in scalar-mediated processes because it is suppressed by powers of velocity.

Since we are finding that downscattering freezes out before depleting the excited states, the DM states have number density

$$n_3 \simeq T^3 \bar{Y} \left( \frac{\xi}{M_\chi} \right) \left( \frac{g_{*S}(T)}{g_{*S}(T_0)} \right), \quad n_1 \simeq T^3 \left( \frac{Y_1}{Y_{\text{tot}}} \right) \left( \frac{\xi}{M_\chi} \right) \left( \frac{g_{*S}(T)}{g_{*S}(T_0)} \right), \quad (28)$$

where  $\xi = 7 \times 10^{-10}$  GeV. We estimate that freezeout occurs at  $\Gamma_{\downarrow} \simeq 3H$ , with  $H \simeq 1.66 \sqrt{g_*(T)} T^2/M_P$ , which should happen before  $e^+e^-$  annihilation. For  $\chi_3 \chi_3 \rightarrow \chi_1 \chi_1$  scattering,

$$T_f = 153 \left( \frac{y^2}{m_\phi^2} - \frac{y_\Phi^2 \eta^2}{m_\Phi^2} \right)^{-2} \frac{1}{\xi M_P \sqrt{M_\chi \delta M_{13}}} \left( \frac{0.33}{\bar{Y}} \right). \quad (29)$$

Requiring  $T_f \gtrsim 5 \delta M_{13}$ , this generically leads to the constraint

$$\max \left( \frac{y}{m_\phi}, \frac{y_\Phi \eta}{m_\Phi} \right) < \frac{1}{15 \text{ GeV}} \left( \frac{10 \text{ GeV}}{M_\chi} \right)^{1/8} \left( \frac{0.33}{\bar{Y}} \right)^{1/4} \left( \frac{3m_e}{\delta M_{13}} \right)^{3/8}, \quad (30)$$

which is easily compatible with the fiducial values  $y \sim 3 \times 10^{-3}$ ,  $m_\phi \sim 4.6$  GeV. It is also compatible with any perturbative value of  $y_\Phi$  for  $m_\Phi \gtrsim$  GeV and  $\eta \sim 10^{-3}$ . Similarly, for

<sup>5</sup> The  $Z'$  fine structure constant has approximately the same functional dependence on  $M_\chi$  as  $\alpha_g$  in [22].

$\chi_3\chi_1 \rightarrow \chi_1\chi_1$  downscattering, we find

$$\max\left(\frac{y\sqrt{\eta}}{m_\phi}, \frac{y_\Phi\sqrt{\eta}}{m_\Phi}\right) < \frac{1}{14 \text{ GeV}} \left(\frac{10 \text{ GeV}}{M_\chi}\right)^{1/8} \left(\frac{0.33}{Y_1/Y_{tot}}\right)^{1/4} \left(\frac{3m_e}{\delta M_{13}}\right)^{3/8}, \quad (31)$$

which is likewise a weak constraint. Finally,  $\chi_3\chi_3 \rightarrow \chi_2\chi_2$  freezeout (which occurs after  $e^+e^-$  annihilation) yields

$$\frac{g}{m_{Z'}} < \frac{1}{3.8 \text{ GeV}} \left(\frac{10 \text{ GeV}}{M_\chi}\right)^{1/8} \left(\frac{0.33}{\bar{Y}}\right)^{1/4} \left(\frac{10 \text{ keV}}{\delta M_{23}}\right)^{3/8}. \quad (32)$$

This is compatible with (10) for our fiducial parameter values, in particular as long as  $\zeta_\downarrow > 350$ , which is a very mild lower limit on the cuspieness of the DM density profile (fig. 2) compared to that expected from  $N$ -body simulations.

#### Kinetic before chemical freezeout?

We have so far assumed that  $\chi_1$  is completely decoupled from  $\chi_{2,3}$  by the chemical freezeout, which necessitated a separate annihilation channel for  $\chi_1$ . If  $\chi_{2,3}$  can efficiently downscatter into  $\chi_1$  during chemical freezeout, then the relic abundance for all three DM species is determined simply by the annihilation and coannihilation of  $\chi_2$  and  $\chi_3$  with subsequent scattering into  $\chi_1$ . In this case, the neutral  $\Phi$  scalar is not necessary and could be eliminated from the model.

Under what conditions could this simplification be achieved? In the absence of the  $\Phi$ , the scattering processes  $\chi_3\chi_3 \leftrightarrow \chi_1\chi_1$  and  $\chi_2\chi_3 \leftrightarrow \chi_2\chi_1$  are parametrically the largest among scatterings mediated by  $\phi$  and  $Z'$  respectively. For them to be in equilibrium during chemical freezeout at  $T \simeq M_\chi/18$ , we require

$$\begin{aligned} \frac{y}{m_\phi} &> \frac{1}{54 \text{ GeV}} \left(\frac{10 \text{ GeV}}{M_\chi}\right)^{3/8} \left(\frac{0.33}{\bar{Y}}\right)^{1/4} \left(\frac{3m_e}{\delta M_{13}}\right)^{1/8} \quad \text{or} \\ \frac{g\sqrt{\eta}}{m_{Z'}} &> \frac{1}{59 \text{ GeV}} \left(\frac{10 \text{ GeV}}{M_\chi}\right)^{3/8} \left(\frac{0.33}{\bar{Y}}\right)^{1/4} \left(\frac{3m_e}{\delta M_{13}}\right)^{1/8}. \end{aligned} \quad (33)$$

The first is clearly ruled out for the parameter ranges of interest. In light of equation (10), the second is also difficult to achieve but may occur for large  $\eta$  corresponding to  $\delta M_{23} \simeq \text{MeV}$ , at the boundary of the allowed parameter space. Apart from this marginal possibility, kinetic freezeout of  $\chi_1$  generically occurs before chemical freezeout.

#### 4.3 Astrophysical Constraints

Light (GeV to 10 GeV mass) dark matter is subject to a number of constraints from astrophysics, which we review briefly here as applied to our model.

The cosmic microwave background (CMB) begins to constrain the possible annihilation channels of light DM. These can inject energy into the SM plasma at redshifts from approximately 100 to 1000, slightly modifying recombination; an inexhaustive list of recent references includes [38–40]. Current limits disfavor DM annihilations primarily to electrons for DM masses  $M_\chi \lesssim 10 \text{ GeV}$  with the standard thermal cross section, but annihilation primarily to muons (or to any other particle whose decay products contain significant numbers of neutrinos) is allowed [38, 39]. For  $Z'$  masses considered here, our models have a branching ratio of about 44% into  $4\mu$  and another 44% into  $2\mu, 2e$  after decay of the  $Z'$  in the  $\chi\chi \rightarrow Z'Z'$  branch. As a result, they are subject to the more relaxed limits. Furthermore, because  $Z'$  is relativistic at thermal freezeout, the annihilation cross section is slightly reduced compared to the canonical value, relaxing the constraints somewhat. In addition, ref. [41] has recently argued that the canonical value of the thermal abundance cross

section should itself be decreased in the vicinity of  $M_\chi = 10$  GeV, again loosening CMB bounds. As a result, our models evade these constraints at present. The effects on the CMB of  $e^+$  production via downscattering are currently under investigation [42].

Diffuse gamma ray emission in our galaxy can similarly be used to place limits on annihilation of DM to SM fermions via final state radiation and inverse Compton scattering. (see, for example [43], for current results). However, these limits are both weaker than those extracted from the CMB and more subject to astrophysical uncertainty.

Dark matter can also affect stellar evolution if it has a large enough capture cross section to accumulate significantly within stars (see [44] and references therein). Only stars orbiting close to the center of our galaxy would be able to capture enough WIMPs to undergo significant effects. With sufficient accumulation, the luminosity from DM annihilations can suppress nuclear burning and increase the star's main-sequence lifetime, with an effect going inversely to the mass of the star. In [44] it was shown that for spin-dependent DM-nucleon scattering cross section  $\sigma_{SD} = 10^{-38}$  cm<sup>2</sup> and mass  $M_\chi = 100$  GeV, and assuming a cuspy DM density profile, these effects could be observable in binary systems in close elliptical orbits around the galactic center. The figure of merit for an observable effect is the ratio of the capture cross section to  $M_\chi$ . For spin-independent scattering, capture on helium is  $\sim 10$  times more effective than spin-dependent capture on hydrogen, but only  $\sim 10/4$  for a model like ours where DM interacts with protons but not neutrons. Thus to be on the borderline for an observable effect, we would need  $\sigma/M_\chi \gtrsim 4 \times 10^{-41}$  cm<sup>2</sup>. In the examples we will discuss in section 5, this criterion is satisfied, and so one could hope to observe binary systems with unusual properties near the galactic center. But at the present, given the great uncertainties in the DM density at the galactic center (in a much smaller region than that over which the positron annihilation for the 511 keV signal is occurring), such considerations cannot yet place a constraint on the model, especially since [44] assumed an NFW profile to obtain their optimistic results, which is more cuspy than the Einasto profile we have assumed.

## 5 Direct detection

There has been much interest in hints of light dark matter from the DAMA [45], CoGeNT [46] and CRESST [47] experiments, supported by evidence of annual modulations in the first two [48]. It is difficult to engineer models with the right properties to fit all sets of observations, but less for only one of them, in particular that of CoGeNT (see for example [49]). The best fit for CoGeNT alone, according to the collaboration's preliminary estimates that take into account contamination due to surface events [50] is  $M_\chi \simeq 10$  GeV and  $\sigma_n = 2 \times 10^{-41}$  cm<sup>2</sup>. This region is excluded by Xenon100 [51], but the edge of the CoGeNT-allowed region at  $M_\chi = 7$  GeV,  $\sigma_n = 5 \times 10^{-41}$  cm<sup>2</sup> is marginally compatible; we will focus on these values. In a model like ours where DM interacts only with protons, one must rescale the cross section by  $(A/Z)^2$  which for Ge is a factor of 5.2, so that the desired cross section on protons is  $\sigma_p = 2.6 \times 10^{-40}$  cm<sup>2</sup>.

The cross section for  $\chi_3$  scattering on protons, mediated by  $Z'$  exchange, is given by

$$\sigma_p = \frac{(g\epsilon\epsilon\mu_N)^2}{\pi m_{Z'}^4} \quad (34)$$

where  $\mu_N$  is the DM-nucleon reduced mass. Using  $M_\chi = 7$  GeV in (13), corresponding to the lowest (and least fine-tuned) relic density contour of fig. 3, we find that  $m_{Z'} = 264$  MeV and  $g = 0.047$ . Then (34) gives the desired value of  $\sigma_p$  to match CoGeNT if

$$\epsilon \simeq 10^{-6} \quad (35)$$

Unfortunately it is difficult to find further complementary evidence for such a weak level of kinetic mixing. It is an order of magnitude below the sensitivity of the Heavy Photon Search (HPS) beam dump experiment proposed at Jefferson Laboratory [52].

However, a DM particle with slightly lower mass  $M_\chi \sim 4$  GeV and larger cross section  $\sigma \sim 5 \times 10^{-39} \text{ cm}^2$  can have a larger value of  $\epsilon$ . These numbers correspond to the best fit for CoGeNT found by ref. [49] for the case of 10% channeling (see fig. 13 of that paper), taking into account our  $(A/Z)^2$  correction factor. Although such a large channeling fraction is not a favored scenario [53], we choose it to illustrate that such values are within reason. In this case, (13) gives  $m_{Z'} = 200$  MeV,  $g = 0.036$ . Then  $\epsilon = 1.5 \times 10^{-3}$ , which is in fact already marginally excluded by recent limits from the MAMI (Mainz Microtron) [54] and APEX [55] experiments. Clearly then, the value of  $\epsilon$  needed to saturate DM direct detection limits is rather sensitive to  $M_\chi$  and there is room for models in which not only the DM itself but also the new mediator particle can be directly observed.

We note that any relic population of  $\chi_1$  particles, even if comparable in number to  $\chi_{2,3}$ , will be undetectable by current direct detection experiments. First, only the elastic scattering  $\chi_1 N \rightarrow \chi_1 N$  mediated by  $\Phi$  is kinematically allowed, and this has cross section (on nucleons)

$$\sigma_N = \frac{(y_\Phi \Theta y_N \mu_N)^2}{\pi m_\Phi^4}, \quad (36)$$

where  $y_N = 0.3m_N/v \approx 1.14 \times 10^{-3}$  is the nucleon-Higgs Yukawa coupling ( $v = 246$  GeV is the Higgs VEV). For  $M_\chi = 7$  GeV and fiducial values for the other parameters as given in table 1, this is  $\sigma_N = 6.3 \times 10^{-46} \text{ cm}^2$ , several orders of magnitude below current experimental limits.

## 6 Conclusions

In this work we have explored the consequences of assuming that the excess galactic 511 keV signal is results from heavy (compared to the MeV scale) dark matter interacting via an abelian gauge interaction. While it will be difficult to demonstrate that this signal is due to dark matter rather than some more mundane astrophysical mechanism, the possibility of having independent discovery of elements of such a model from direct detection of the dark matter or of the dark gauge boson could make such an identification more plausible. (Higher resolution measurements of the morphology of the 511 keV signal by a future low-energy  $\gamma$ -ray mission would also help to settle this question.) Conversely, the ability to exclude part of the parameter space by independent experiments is an interesting feature of this type of model. The model we have presented with the fiducial parameter values listed in table 1 gives an existence proof that abelian DM can produce enough positrons to explain the 511 keV signal as well as avoid known constraints and potentially provide independent signals.

This model, having three components of dark matter and two new Higgs bosons, is surprisingly rich, including some complications necessitated by the many constraints which must be satisfied: naturally small mass splittings, a long-lived excited state, short-lived intermediate state, and correct relic densities of the three DM species. Perhaps the most peculiar feature of the model is an accidental near-degeneracy of the DM mass parameters  $M_\chi$  and  $m$  such that  $M_\chi - m \gtrsim 2m_e$ . It should be emphasized that this is not a fine-tuning in the usual sense since the fermion masses are protected by chiral symmetry and therefore the MeV-scale splitting is not destabilized by radiative corrections. A more complete theory would presumably give an explanation for this mass difference, just as the eventual successor to the standard model of particle physics will hopefully explain why  $m_e$  is much smaller than the mass of the top quark.

As a compensation for its lack of elegance, we find that the model can have interesting predictions for direct detection in the regions suggested by CoGeNT and CRESST (or lower masses  $\sim 4$  GeV), and possibly for beam-dump searches for light vector bosons such as the APEX, MAMI and HPS experiments. The dark Higgs boson  $\Phi$  could moreover mix with the standard model Higgs boson and manifest itself through invisible decays of the latter.



**Acknowledgements** This work was supported in part by the Natural Sciences and Engineering Research Council of Canada.

## References

- [1] O. Adriani *et al.*, Nature **458**, 607–609 (2009).
- [2] A. A. Abdo *et al.*, Phys.Rev.Lett. **102**, 181101 (2009).
- [3] W. N. Johnson III., F. R. Harnden Jr., and R. C. Haymes, Astrophys.J. **172**(February), L1 (1972).
- [4] M. Leventhal, C. J. MacCallum, and P. D. Stang, Astrophys.J.Lett. **225**(October), L11–L14 (1978).
- [5] J. Knodlseder, V. Lonjou, P. Jean, M. Allain, P. Mandrou *et al.*, Astron.Astrophys. **411**, L457–L460 (2003).
- [6] P. Jean, J. Knodlseder, V. Lonjou, M. Allain, J. P. Roques *et al.*, Astron.Astrophys. **407**, L55 (2003).
- [7] J. Knodlseder, P. Jean, V. Lonjou, G. Weidenspointner, N. Guessoum *et al.*, Astron.Astrophys. **441**, 513–532 (2005).
- [8] L. Bouchet, E. Jourdain, J. Roques, A. Strong, R. Diehl *et al.*(2008).
- [9] W. Wang, C. Pun, and K. Cheng, Astron.Astrophys. **446**, 943–948 (2006).
- [10] M. Casse, B. Cordier, J. Paul, and S. Schanne, Astrophys.J. **602**, L17–L20 (2004).
- [11] G. Bertone, A. Kusenko, S. Palomares-Ruiz, S. Pascoli, and D. Semikoz, Phys.Lett. **B636**, 20–24 (2006).
- [12] P. Milne, J. Kurfess, R. Kinzer, and M. Leising, New Astron.Rev. **46**, 553–558 (2002).
- [13] K. Ahn, E. Komatsu, and P. Hoflich, Phys.Rev. **D71**, 121301 (2005).
- [14] K. Cheng, D. Chernyshov, and V. Dogiel, Astrophys.J. **645**, 1138–1151 (2006).
- [15] G. Weidenspointner, G. Skinner, P. Jean, J. Knodlseder, P. von Ballmoos *et al.*, Nature **451**, 159–162 (2008).
- [16] A. Calvez and A. Kusenko, Phys.Rev. **D82**, 063005 (2010).
- [17] J. Higdon, R. Lingenfelter, and R. Rothschild, Astrophys.J. **698**, 350–379 (2009).
- [18] R. Lingenfelter, J. Higdon, and R. Rothschild, Phys.Rev.Lett. **103**, 031301 (2009).
- [19] R. M. Bandyopadhyay, J. Silk, J. E. Taylor, and T. J. Maccarone(2008).
- [20] N. Prantzos, C. Boehm, A. Bykov, R. Diehl, K. Ferriere *et al.*, Reviews of Modern Physics **83**, 1001–1056 (2011).
- [21] P. Martin, A. Strong, P. Jean, A. Alexis, and R. Diehl(2012).
- [22] J. M. Cline, A. R. Frey, and F. Chen, Phys.Rev. **D83**, 083511 (2011).
- [23] A. C. Vincent, P. Martin, and J. M. Cline, JCAP (to appear) (2012).
- [24] D. P. Finkbeiner and N. Weiner, Phys.Rev. **D76**, 083519 (2007).
- [25] M. Pospelov and A. Ritz, Phys.Lett. **B651**, 208–215 (2007).
- [26] N. Arkani-Hamed, D. P. Finkbeiner, T. R. Slatyer, and N. Weiner, Phys.Rev. **D79**, 015014 (2009).
- [27] D. P. Finkbeiner, T. R. Slatyer, N. Weiner, and I. Yavin, JCAP **0909**, 037 (2009).
- [28] F. Chen, J. M. Cline, and A. R. Frey, Phys.Rev. **D79**, 063530 (2009).
- [29] F. Chen, J. M. Cline, A. Fradette, A. R. Frey, and C. Rabideau, Phys.Rev. **D81**, 043523 (2010).
- [30] R. Morris and N. Weiner, arXiv:1109.3747 (2011).
- [31] C. Picciotto and M. Pospelov, Phys.Lett. **B605**, 15–25 (2005).
- [32] C. Boehm, D. Hooper, J. Silk, M. Casse, and J. Paul, Phys.Rev.Lett. **92**, 101301 (2004).
- [33] D. Hooper, F. Ferrer, C. Boehm, J. Silk, J. Paul *et al.*, Phys.Rev.Lett. **93**, 161302 (2004).
- [34] J. H. Huh, J. E. Kim, J. C. Park, and S. C. Park, Phys.Rev. **D77**, 123503 (2008).
- [35] C. Boehm, T. Delahaye, and J. Silk, Phys.Rev.Lett. **105**, 221301 (2010).
- [36] Z. Abidin, A. Afanasev, and C. E. Carlson(2010).
- [37] F. Chen, J. M. Cline, and A. R. Frey, Phys.Rev. **D80**, 083516 (2009).
- [38] S. Galli, F. Iocco, G. Bertone, and A. Melchiorri, Phys.Rev. **D84**, 027302 (2011).
- [39] G. Hutsi, J. Chluba, A. Hektor, and M. Raidal, Astron.Astrophys. **535**, A26 (2011).
- [40] D. P. Finkbeiner, S. Galli, T. Lin, and T. R. Slatyer, Phys.Rev. **D85**, 043522 (2012).
- [41] G. Steigman, B. Dasgupta, and J. F. Beacom(2012).
- [42] A. R. Frey and N. Reid(work in progress).
- [43] T. F. M. Ackermann *et al.*(2012).
- [44] P. Scott, M. Fairbairn, and J. Edsjo, Mon.Not.Roy.Astron.Soc. **394**, 82 (2009).
- [45] R. Bernabei *et al.*, Eur.Phys.J. **C56**, 333–355 (2008).
- [46] C. Aalseth *et al.*, Phys.Rev.Lett. **106**, 131301 (2011).
- [47] G. Angloher, M. Bauer, I. Bavykina, A. Bento, C. Bucci *et al.*(2011).



- [48] C. Aalseth, P. Barbeau, J. Colaresi, J. Collar, J. Diaz Leon *et al.*, Phys.Rev.Lett. **107**, 141301 (2011).
- [49] M. Farina, D. Pappadopulo, A. Strumia, and T. Volansky, JCAP **1111**, 010 (2011).
- [50] J. Collar, TAUP 2011 presentation.
- [51] E. Aprile *et al.*, Phys.Rev.Lett. **107**, 131302 (2011).
- [52] A. Grillo *et al.*, [http://www.jlab.org/exp\\_prog/proposals/11/PR12-11-006.pdf](http://www.jlab.org/exp_prog/proposals/11/PR12-11-006.pdf).
- [53] N. Bozorgnia, G.B. Gelmini, and P. Gondolo, JCAP **1011**, 028 (2010).
- [54] H. Merkel *et al.*, Phys.Rev.Lett. **106**, 251802 (2011).
- [55] S. Abrahamyan *et al.*, Phys.Rev.Lett. **107**, 191804 (2011).